2020

Sparsity-Based Robust Bistatic MIMO Radar Imaging in the Presence of Array Errors

Wenyu Gao

Jun Li

Daming Zhang

Qinghua Guo
University of Wollongong, qguo@uow.edu.au

Sparsity-Based Robust Bistatic MIMO Radar Imaging in the Presence of Array Errors

Abstract

© 2020 Wenyu Gao et al. A sparse recovery method for robust transmit-receive angle imaging in a bistatic MIMO radar is proposed to deal with the effect of array gain-phase errors. The impact of multiplicative array gain-phase errors is changed to be additive through model reformulation, and transmit-receive angle imaging is formulated to a sparse total least square signal problem. Then, an iterative algorithm is proposed to solve the optimization problem. Compared with existing methods, the proposed method can achieve a significant performance gain in the case that the number of snapshots is small. Simulation results verify the effectiveness of the proposed method.

Publication Details

W. Gao, J. Li, D. Zhang & Q. Guo, "Sparsity-Based Robust Bistatic MIMO Radar Imaging in the Presence of Array Errors," International Journal of Antennas and Propagation, vol. 2020, 2020.

Hindawi
International Journal of Antennas and Propagation
Volume 2020, Article ID 2304913, 8 pages
https://doi.org/10.1155/2020/2304913

Research Article

Sparsity-Based Robust Bistatic MIMO Radar Imaging in the Presence of Array Errors

Wenyu Gao,[1] Jun Li,[1] Daming Zhang,[1] and Qinghua Guo[2]

[1]*National Lab of Radar Signal Processing, Xidian University, Xi'an 710071, China*
[2]*School of Electrical Computer and Telecommunications Engineering, University of Wollongong, Wollonogng 2522, Australia*

Correspondence should be addressed to Jun Li; junli01@mail.xidian.edu.cn

Received 27 May 2019; Revised 16 December 2019; Accepted 31 January 2020; Published 27 February 2020

Academic Editor: Xiulong Bao

A sparse recovery method for robust transmit-receive angle imaging in a bistatic MIMO radar is proposed to deal with the effect of array gain-phase errors. The impact of multiplicative array gain-phase errors is changed to be additive through model reformulation, and transmit-receive angle imaging is formulated to a sparse total least square signal problem. Then, an iterative algorithm is proposed to solve the optimization problem. Compared with existing methods, the proposed method can achieve a significant performance gain in the case that the number of snapshots is small. Simulation results verify the effectiveness of the proposed method.

1. Introduction

Multiple-input multiple-output (MIMO) radars use multiple channels to transmit orthogonal waveforms and multiple channels to receive echo signals, where the transmitting aperture can be fully exploited [1–6]. Compared to a conventional phased-array radar, an MIMO radar can enhance spatial resolution, improve target detection performance, etc. The performance of the MIMO radar can usually be improved by increasing the number of channels. According to the transmitting and receiving antenna configurations, there are two main classes of MIMO radars. The first class is the statistical MIMO radar [7, 8], where transmitting and receiving antennas are widely separated. By exploiting the spatial diversity, the statistical MIMO radar can resist the performance degradations caused by target scintillations. The second class is the colocated MIMO radar [2], where the transmitting antennas and receiving antennas are closely spaced, and performance gain can be achieved by multichannel coherent processing. A colocated MIMO radar can obtain a virtual aperture larger than its real aperture, resulting in lower sidelobes and a narrower beam width.

A bistatic MIMO radar, firstly proposed in [3], has the advantages of both the bistatic radar and the MIMO radar. In the bistatic MIMO radar, the direction of arrival (DOA) and the direction of departure (DOD) of targets can be obtained at the same time by processing the received signals, and it has been employed to identify and locate multiple targets [9, 10], clutter cancellation [11, 12], and imaging [13–15]. Nevertheless, due to the presence of the gain and phase errors of the transmitting array and receiving array, the imaging quality and detection accuracy of these techniques can deteriorate seriously. Many methods have been investigated to mitigate the impact of array gain-phase errors in the bistatic MIMO radar [16, 17]. However, these methods work well with a large number of snapshots, but they do not work properly when the number of snapshots is small.

Sparse recovery techniques [18–20] can be employed to achieve high-resolution imaging with a small number of samples, and they have been applied to bistatic MIMO radar imaging. A sparse recovery-based imaging method is proposed in [14], which is robust to large gain errors. However, the method does not consider the array phase errors and does not work well with a single snapshot. In [15], a transmit-receive angle imaging method is proposed, but its complexity is high and its performance degrades severely when the gain-phase errors are relatively large. In this work, we propose a robust sparse recovery method for transmit-

receive angle imaging in the bistatic MIMO radar. Signals are transformed into a sparse domain by discrete wavelet transform. Then, the reconstruction is formulated as an optimization problem which is solved iteratively. The proposed method is more robust in dealing with the imperfection of array gain-phase errors and noise in the bistatic MIMO radar system. We analyse the key parameters affecting the performance of recovery results. We also analyse the influence of the number of iterations on the convergence of the algorithm. Simulation results show that compared with existing methods, the proposed method exhibits better robustness.

This paper is organized as follows: The bistatic MIMO radar sparse signal model with array gain-phase errors is derived in Section 2. In Section 3, a robust iterative algorithm is proposed to achieve target image reconstruction in the presence of array gain-phase errors. In Section 4, the effectiveness of the proposed method is verified by simulations. Some conclusions are drawn in Section 5.

2. Signal Model with Array Gain-Phase Errors

We consider a bistatic MIMO radar system with M transmitting antennas and N receiving antennas, where both the transmitter and the receiver are equipped with a uniform linear array (ULA). The transmitted pulses are denoted by $\mathbf{S} \in C^{M\times L}$, where M is the number of coded periodic signals and L is the length of the coding sequence in one pulse period.

As shown in Figure 1, the location of a target can be determined by its angle pair (φ_t, θ_r), where φ_t and θ_r are the angles of the target with respect to the transmitting array and the receiving array, respectively. The received signal can be expressed as

$$Y_q = A_R D_q A_T^T S + E_q, \quad q = 1, 2, \ldots, Q, \tag{1}$$

where $\mathbf{A}_T = [\mathbf{a}_{t1}, \mathbf{a}_{t2}, \ldots, \mathbf{a}_{\mathrm{tg}}, \ldots, \mathbf{a}_{\mathrm{tG}}]_{M\times G}$ and $\mathbf{A}_R = [\mathbf{a}_{r1}, \mathbf{a}_{r2}, \ldots, \mathbf{a}_{\mathrm{rg}}, \ldots, \mathbf{a}_{\mathrm{rG}}]_{N\times G}$ are the steering matrices of the transmitting array and receiving array with G pixel points, $(\cdot)^T$ denotes the transpose operator, and $\mathbf{D}_q = \mathrm{diag}(d_1, \ldots, d_g)$ is a diagonal matrix with diagonal elements being the target scattering coefficients for the qth pulse period. It is assumed that the transmitted signals are orthogonal, i.e., $\mathbf{S}\mathbf{S}^H = \mathbf{I}$, and $\mathbf{E}_q$ denotes complex Gaussian distributed noise with zero mean and $\sigma_n^2\mathbf{I}_N$ covariance. The steering vectors of the receiving array $\mathbf{a}_{\mathrm{rg}}$ and the transmitting array $\mathbf{a}_{\mathrm{tg}}$ can be expressed as

$$\begin{aligned}
\mathbf{a}_{\mathrm{rg}} &= \left[1, e^{j(2\pi/\lambda)d_r \sin\theta_{\mathrm{rg}}}, e^{j(2\pi/\lambda)2d_r \sin\theta_{\mathrm{rg}}}, \ldots, e^{j(2\pi/\lambda)(N-1)d_r \sin\theta_{\mathrm{rg}}}\right]^T,\\
\mathbf{a}_{\mathrm{tp}} &= \left[1, e^{j(2\pi/\lambda)d_t \sin\varphi_{\mathrm{tg}}}, e^{j(2\pi/\lambda)2d_t \sin\varphi_{\mathrm{tg}}}, \ldots, e^{j(2\pi/\lambda)(M-1)d_t \sin\varphi_{\mathrm{tg}}}\right]^T,
\end{aligned} \tag{2}$$

where λ is the signal wavelength and d_t and d_r denote the transmitting antenna spacing and receiving antenna spacing, respectively.

Consider the region of interest Ω, as shown in Figure 1, and we divide it into two-dimensional grids consisting of angular position pairs $\Omega = \{(\varphi_k, \theta_l)\colon (k,l) \in \{1, \ldots, G\} \times \{1, \ldots, G\}\}$. After match filtering by the transmitted waveforms, the received signals turn into

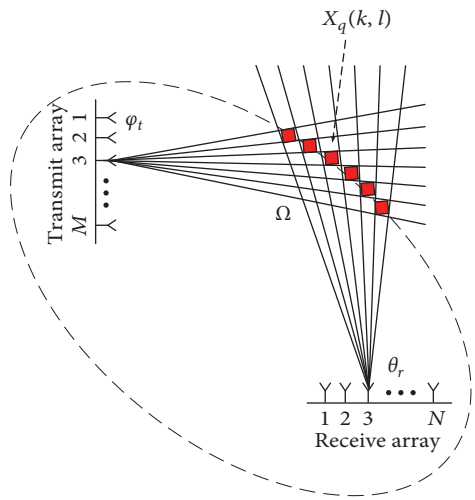

Figure 1: Bistatic MIMO radar imaging.

$$\mathbf{Y}_q = \mathbf{A}_R \mathbf{X}_q \mathbf{A}_T + \mathbf{E}_q, \tag{3}$$

where $\mathbf{X}_q \in \mathbb{C}^{G\times G}$ is the matrix of target pixel distribution and is nonzero only when it is the pixel of the target. When we process the data of one range cell, only surface of the ellipse has the pixels of the target, and any other grid points in Ω are zeros. We can recover the image range by range. The vectorized $\mathbf{Y}_q$ can be expressed as

$$\mathbf{y}_{\mathbf{q}} = \mathrm{vec}\left(\mathbf{Y}_q\right) = \left[\mathbf{A}_R \otimes \mathbf{A}_T\right]\mathrm{vec}\left(\mathbf{X}_q\right) + \mathbf{e}_{\mathbf{q}} = \Phi x'_{\mathbf{q}} + \mathbf{e}_{\mathbf{q}}, \tag{4}$$

where $\mathbf{\Phi}' = \mathbf{A}_R \otimes \mathbf{A}_T$, $\mathbf{x}'_q = \mathrm{vec}(\mathbf{X}_q)$, $\mathbf{e}_q = \mathrm{vec}(\mathbf{E}_q)$, and $\otimes$ denotes the Kronecker product. With the presence of gain-phase errors in the transmitting and receiving arrays, the steering matrices can be represented as

$$\begin{aligned}
\mathbf{\Gamma}_R &= \mathbf{\Theta}'_R \mathbf{A}_R = (\mathbf{I} + \mathbf{\Theta}_R)\mathbf{A}_R = \mathbf{A}_R + \mathbf{\Theta}_R \mathbf{A}_R = \mathbf{A}_R + \mathbf{\Delta S}_R,\\
\mathbf{\Gamma}_T &= \mathbf{\Theta}'_T \mathbf{A}_T = (\mathbf{I} + \mathbf{\Theta}_T)\mathbf{A}_T = \mathbf{A}_T + \mathbf{\Theta}_T \mathbf{A}_T = \mathbf{A}_T + \mathbf{\Delta S}_T,
\end{aligned} \tag{5}$$

where $\mathbf{\Theta}_R = \mathrm{diag}(\sigma_{R1}, \ldots, \sigma_{\mathrm{RN}})$ and $\mathbf{\Theta}_T = \mathrm{diag}(\sigma_{T1}, \ldots, \sigma_{\mathrm{TM}})$ are the diagonal matrices containing gain-phase errors. The diagonal elements $\sigma_{\mathrm{Ri}} = a_{\mathrm{Ri}} e^{j\varphi_{\mathrm{Ri}}}$ and $\sigma_{\mathrm{Ti}} = a_{\mathrm{Ti}} e^{j\varphi_{\mathrm{Ti}}}$, where a_{Ri} and a_{Ti} denote the gain errors of the receiving array and transmitting array elements and φ_{Ri} and φ_{Ti} denote the phase errors of the receiving array and transmitting array elements, respectively. The received signal with the gain-phase errors can be expressed as

$$\mathbf{Z}_q = \mathbf{\Gamma}_R \mathbf{X}_q \mathbf{\Gamma}_T + \mathbf{E}_q. \tag{6}$$

Hence, the vector form of equation (6) can be written as

$$\begin{aligned}\mathbf{z_q} &= \mathrm{vec}\left(\mathbf{Z}_q\right) = \left[\mathbf{\Gamma}_R \otimes \mathbf{\Gamma}_T\right]\mathrm{vec}\left(\mathbf{X}_q\right) + \mathbf{e_q} = \left[\left(\mathbf{A}_R + \Delta\mathbf{S}_R\right)\right. \\ &\quad \left.\otimes \left(\mathbf{A}_T + \Delta\mathbf{S}_T\right)\right]\mathbf{x}_\mathbf{q}' + \mathbf{e_q} \\ &= \left[\mathbf{A}_R \otimes \mathbf{A}_T + \Delta\mathbf{S}_R \otimes \mathbf{A}_T + \mathbf{A}_R \otimes \Delta\mathbf{S}_T\right. \\ &\quad \left. + \Delta\mathbf{S}_R \otimes \Delta\mathbf{S}_T\right]\mathbf{x}_\mathbf{q}' + \mathbf{e_q} = \left(\mathbf{\Phi}' + \Delta\mathbf{v}'\right)\mathbf{x}_\mathbf{q}' + \mathbf{e_q},\end{aligned} \tag{7}$$

where $\Delta\mathbf{v}' = \Delta\mathbf{S}_R \otimes \mathbf{A}_T + \mathbf{A}_R \otimes \Delta\mathbf{S}_T + \Delta\mathbf{S}_R \otimes \Delta\mathbf{S}_T$ can be modeled as an additive random perturbation matrix on the ideal measurement matrix $\mathbf{\Phi}'$. We use the symlet wavelet in discrete wavelet transform (DWT), to transform the image into a sparse domain, and then reconstruct the image with our robust algorithms in the sparse domain. We assume that the wavelet transform matrix is $W \in \mathbb{C}^{G\times G}$ and then $W\mathbf{x}_\mathbf{q}' = \mathbf{x_q}$, so $\mathbf{x_q}$ is a representation of $\mathbf{x}_\mathbf{q}'$ in the sparse domain. Accordingly, equation (7) can be rewritten as

$$\begin{aligned}\mathbf{z_q} &= \left(\mathbf{\Phi}' + \Delta\mathbf{v}'\right)\mathbf{x}_\mathbf{q}' + \mathbf{e_q} = \left(\mathbf{\Phi}' + \Delta\mathbf{v}'\right)\mathbf{W}^{-1}\mathbf{x_q} \\ &\quad + \mathbf{e_q} = \left(\mathbf{\Phi} + \Delta\mathbf{v}\right)\mathbf{x_q} + \mathbf{e_q},\end{aligned} \tag{8}$$

where $\mathbf{\Phi} = \mathbf{\Phi}'\mathbf{W}^{-1}$ and $\Delta\mathbf{v} = \Delta\mathbf{v}'\mathbf{W}^{-1}$. The objective is to recover the sparse vector $\mathbf{x_q}$, which is elaborated in Section 3.

3. Iterative Sparse Recovery Imaging Algorithm

The model $\mathbf{z}_q = \left(\mathbf{\Phi} + \Delta\mathbf{v}\right)\mathbf{x}_q + \mathbf{e}_q$ shown in (8) considers both gain-phase errors and noise. The optimization problem with the sparsity constraint can be formulated as [20]

$$\begin{aligned}\left\{\mathbf{x_q}, \Delta\mathbf{v}, \mathbf{e_q}\right\} &= \arg\min_{\mathbf{x},\Delta\mathbf{v},\mathbf{e_q}} \left\|\left[\Delta\mathbf{v}, \mathbf{e_q}\right]\right\|_\mathrm{F}^2 + \gamma\left\|\mathbf{x_q}\right\|_1 \\ &\quad \text{s.t. } \mathbf{z_q} = \left(\mathbf{\Phi} + \Delta\mathbf{v}\right)\mathbf{x_q} + \mathbf{e_q}.\end{aligned} \tag{9}$$

The cost function includes two parts: the error term $\|\Delta\mathbf{v}, \mathbf{e}_q\|_F^2$ and the regularization term $\gamma\|\mathbf{x}_q\|_1$, where γ is a regularization parameter to control the sparsity of the solution. In the problem formulated in (9), the observation vector $\mathbf{z}_q$ and measurement matrix $\mathbf{\Phi}$ are given and $\Delta\mathbf{v}$ and $\mathbf{e}_q$ are the unknown perturbation matrix and noise vector, respectively. Our aim is to recover the unknown signal vector $\mathbf{x}_q$, which is a nonconvex optimization problem.

We use a coordinate descent method to solve the optimization problem. In the ith iteration, the method performs two steps. In the first step, $\mathbf{x}_q$ is updated, which can be formulated as

$$\mathbf{x_q}(i) = \arg\min_{\mathbf{x_q}} \left\|\mathbf{z_q} - \left(\mathbf{\Phi} + \Delta\mathbf{v}(i-1)\right)\mathbf{x_q}\right\|_2^2 + \gamma\left\|\mathbf{x_q}\right\|_1, \tag{10}$$

where the matrix $\Delta\mathbf{v}(i-1)$ is obtained in the last iteration, and the optimization problem above is convex. The second step is to update the perturbation matrix $\Delta\mathbf{v}$ with $\mathbf{x}_q(i)$ obtained in the first step, i.e.,

$$\Delta\mathbf{v}(i) = \arg\min_{\Delta\mathbf{v}} \left\|\mathbf{z_q} - \left(\mathbf{\Phi} + \Delta\mathbf{v}\right)\mathbf{x_q}(i)\right\|_2^2 + \|\Delta\mathbf{v}\|_F^2. \tag{11}$$

The method fixes a parameter between $\mathbf{x}_q$ and $\Delta\mathbf{v}$ while optimizing the other one, until a stop criterion is satisfied. In each iteration, $\mathbf{x}_q$ can be solved by the following optimization problem [21]:

$$\begin{aligned}\mathbf{x_q}(i) &= \arg\min_{\mathbf{x_q},\mathbf{w}} \frac{1}{2}\left\|\mathbf{z_q} - \left(\mathbf{\Phi} + \Delta\mathbf{v}\right)\mathbf{x_q}\right\|_2^2 + \gamma\|\mathbf{w}\|_1 \\ &\quad + \frac{\rho}{2}\left\|\mathbf{x_q} - \mathbf{w}\right\|_2^2, \\ &\quad \text{s.t. } \mathbf{x_q} - \mathbf{w} = 0.\end{aligned} \tag{12}$$

In the above, we add the penalty term $\rho/2\|\mathbf{x}_q - \mathbf{w}\|_2^2$ to bring robustness to the dual ascent method, where ρ is a penalty parameter. Then, we can form the augmented Lagrangian:

$$\begin{aligned}\Lambda\left(\mathbf{x_q}, \mathbf{w}, \mathbf{L}\right) &= \frac{1}{2}\left\|\mathbf{z_q} - \left(\mathbf{\Phi} + \Delta\mathbf{v}\right)\mathbf{x_q}\right\|_2^2 + \gamma\|\mathbf{w}\|_1 + \frac{\rho}{2}\left\|\mathbf{x_q} - \mathbf{w}\right\|_2^2 \\ &\quad + \mathbf{L}^\mathrm{T}\left(\mathbf{x_q} - \mathbf{w}\right),\end{aligned} \tag{13}$$

where the constraint s.t. $\mathbf{x}_q - \mathbf{w} = 0$ can be written as the term $\mathbf{L}^T(\mathbf{x}_q - \mathbf{w})$ and L is a Lagrangian multiplier vector. We use the alternating iteration method to solve (13). In the $k+1$th iteration, the method performs three steps. In the first step, $\mathbf{x}_q$ can be updated as

$$\mathbf{x}_\mathbf{q}^{k+1} = \arg\min_{\mathbf{x_q}} \Lambda\left(\mathbf{x_q}, \mathbf{w}^\mathrm{k}, \mathbf{L}^\mathrm{k}\right). \tag{14}$$

By calculating the partial derivative of $\Lambda(\mathbf{x}_q, \mathbf{w}^\mathbf{k}, \mathbf{L}^\mathbf{k})$ with respect to $\mathbf{x}_q$ and making it equal to zero, we can update $\mathbf{x_q}$ as

$$\mathbf{x}_\mathbf{q}^{k+1}(i) = \left(\left(\mathbf{\Phi} + \Delta\mathbf{v}\right)^T\left(\mathbf{\Phi} + \Delta\mathbf{v}\right) + \rho\mathbf{I}\right)^{-1}\left(\left(\mathbf{\Phi} + \Delta\mathbf{v}\right)^T\mathbf{z_q} + \rho\mathbf{w}^k - \mathbf{L}^k\right), \tag{15}$$

where $\mathbf{w}$ and $\mathbf{L}$ are fixed and $\left(\mathbf{\Phi} + \Delta\mathbf{v}\right)^T\left(\mathbf{\Phi} + \Delta\mathbf{v}\right) + \rho\mathbf{I}$ is always invertible since $\rho > 0$. Then, $\mathbf{w}$ can be updated by

$$\mathbf{w}^{k+1} = \arg\min_{\mathbf{w}} \Lambda\left(\mathbf{x}_\mathbf{q}^{k+1}(i), \mathbf{w}, \mathbf{L}^k\right). \tag{16}$$

Similarly, we can get $\mathbf{w}^{k+1}$ by letting the partial derivative of $\Lambda(\mathbf{x}_q^{k+1}(i), \mathbf{w}, \mathbf{L}^k)$ with respect to $\mathbf{w}$ equal to zero, i.e.,

$$\mathbf{w}^{k+1} = \mathrm{sign}\left(\mathbf{x}_\mathbf{q}^{k+1}(i) + \frac{\mathbf{L}^k}{\rho}\right) \odot \max\left(\left|\mathbf{x}_\mathbf{q}^{k+1}(i) + \frac{\mathbf{L}^k}{\rho}\right| - \frac{\gamma}{\rho}, 0\right), \tag{17}$$

where $\mathbf{x}_q^{k+1}(i)$ and $\mathbf{L}^k$ are fixed and $\odot$ denotes point multiplication. The updated estimates of $\mathbf{x}_q^{k+1}(i)$ and $\mathbf{w}^{k+1}$ are then employed to update the current estimate of $\mathbf{L}^{k+1}$:

$$\mathbf{L}^{k+1} = \mathbf{L}^k + \rho\left(\mathbf{x}_\mathbf{q}^{k+1}(i) - \mathbf{w}^{k+1}\right), \tag{18}$$

with $\mathbf{x}_q(i)$ available, the above formula is quadratic. Then, letting the first-order derivative of (11) with respect to $\Delta\mathbf{v}$ to be zero, we have

$$\Delta\mathbf{v}(i) = \left(\mathbf{z_q} - \mathbf{\Phi}\mathbf{x_q}\right)\mathbf{x}_\mathbf{q}^T(i)\left(\mathbf{x_q}(i)\mathbf{x}_\mathbf{q}^T(i) + \mathbf{I}\right)^{-1}. \tag{19}$$

The proposed algorithm is given in Algorithm 1.

Input: $\mathbf{z}_q$, $\mathbf{\Phi}$, γ, ρ
Output: $\mathbf{x}_q$, $\Delta\mathbf{v}$
Initialization with $\Delta\mathbf{v}(\mathbf{0}) = \mathbf{0}_{M\times N}$, $\mathbf{w} = \mathbf{0}_{N\times 1}$, $\mathbf{L} = \mathbf{0}_{1\times N}$, and $\mathrm{err}(0) = 0$
for $i = 1, 2, \ldots, m$ **do**
  for $k = 0, \ldots, n$ **do**
   Update the iterate $\mathbf{x}_q^{k+1}$ as
    $$\mathbf{x}_\mathbf{q}^{k+1}(i) = ((\mathbf{\Phi} + \Delta\mathbf{v})^T(\mathbf{\Phi} + \Delta\mathbf{v}) + \rho\mathbf{I})^{-1}((\mathbf{\Phi} + \Delta\mathbf{v})^T\mathbf{z}_\mathbf{q} + \rho\mathbf{w}^k - \mathbf{L}^k)$$
   Compute the vector $\mathbf{w}^{k+1}$ as
    $$\mathbf{w}^{k+1} = \mathrm{sign}(\mathbf{x}_\mathbf{q}^{k+1}(i) + \mathbf{L}/\rho) \odot \max(|\mathbf{x}_\mathbf{q}^{k+1}(i) + \mathbf{L}/\rho| - \gamma/\rho, 0)$$
   Update $\mathbf{L}^{k+1}$ as
    $$\mathbf{L}^{k+1} = \mathbf{L}^k + \rho(\mathbf{x}_\mathbf{q}^{k+1}(i) - \mathbf{w}^{k+1})$$
  end for
  Update the perturbation matrix $\Delta\mathbf{v}(i)$ as
    $$\Delta\mathbf{v}(i) = (\mathbf{z}_\mathbf{q} - \mathbf{\Phi}\mathbf{x}_\mathbf{q})\mathbf{x}_\mathbf{q}^T(i)(\mathbf{x}_\mathbf{q}(i)\mathbf{x}_\mathbf{q}^T(i) + \mathbf{I})^{-1}$$
  Update the squared l_2 error $\mathrm{err}(i)$ as
    $$\mathrm{err}(i) = \|\mathbf{z}_\mathbf{q} - [\mathbf{\Phi} + \Delta\mathbf{v}(i)]\mathbf{x}_\mathbf{q}(i)\|_2^2$$
  if $|\mathrm{err}(i) - \mathrm{err}(i-1)| \le \delta$
    break
  end if
end for

Algorithm 1: Proposed algorithm flow.

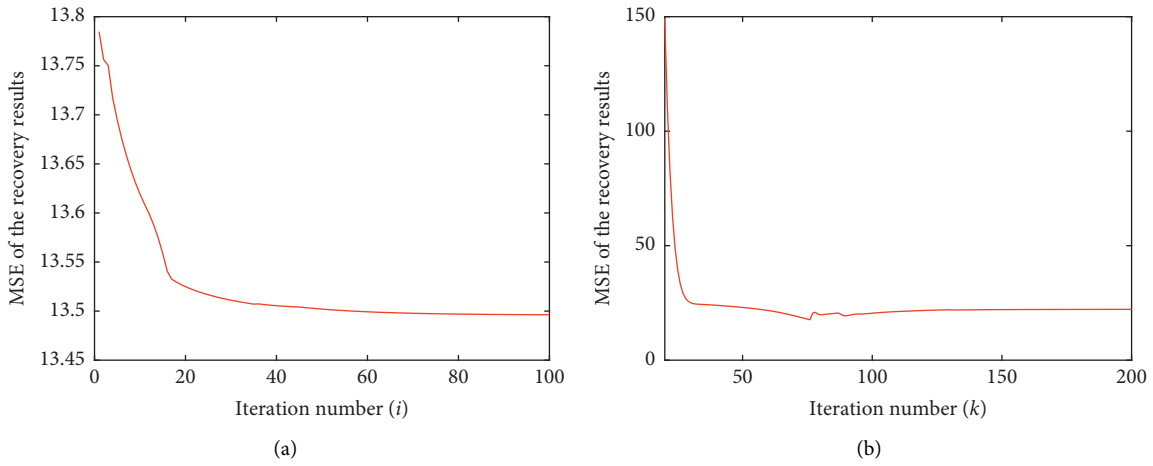

Figure 2: MSE of the reconstruction results with different numbers of iterations of i and k when $M = N = 15$ and SNR = 20 dB. (a) MSE with the iteration number i when $k = 200$. (b) MSE with the iteration number k when $i = 60$.

We set the regularization parameter γ as 15 and penalty parameter ρ as 0.2. The algorithm stops when the difference of the squared l_2 error of two consecutive iterations is less than $\delta = 1e^{-10}$. After obtaining $\mathbf{x}_\mathbf{q}$, we use $\mathbf{x}_\mathbf{q}' = \mathbf{W}^{-1}\mathbf{x}_\mathbf{q}$ to transform x_q to $\mathbf{x}_\mathbf{q}'$ to obtain the reconstructed image. The computational complexity of the proposed algorithm is $\mathcal{O}((N^3)G)$, where N is the number of receiving antennas and $G = mn$ denotes the product of two iteration numbers. Generally, $G = 200$ will lead to satisfactory quality of the reconstructed image.

4. Simulation Results

In this section, we examine the performance of the proposed method in comparison with that of the Lasso method and the methods proposed in [14] and [15]. We use the mean square error (MSE) and performance recovery coefficient (PRC) with the following definitions to evaluate the reconstruction quality:

$$\mathrm{MSE} = \left\|\mathbf{x}_\mathbf{q}' - \mathbf{x}_\mathbf{t}\right\|_2^2,$$
$$\mathrm{PRC} = \frac{\left|\left(\mathbf{x}_\mathbf{q}'\right)^T\mathbf{x}_\mathbf{t}\right|}{\left\|\mathbf{x}_\mathbf{q}'\right\|_2\left\|\mathbf{x}_\mathbf{t}\right\|_2}, \tag{20}$$

where $\mathbf{x}_t$ represents the true image and $\mathbf{x}_q'$ denotes the reconstructed image. The PRC measures the similarity of the true target coefficient and the estimated target coefficient. Generally, the larger the PRC, the smaller the MSE and the better the quality of the reconstructed image.

In our simulations, both the transmitting array and receiving array are ULAs with 15 elements and half-wavelength spacing. There are 64 pixels in each range. In each

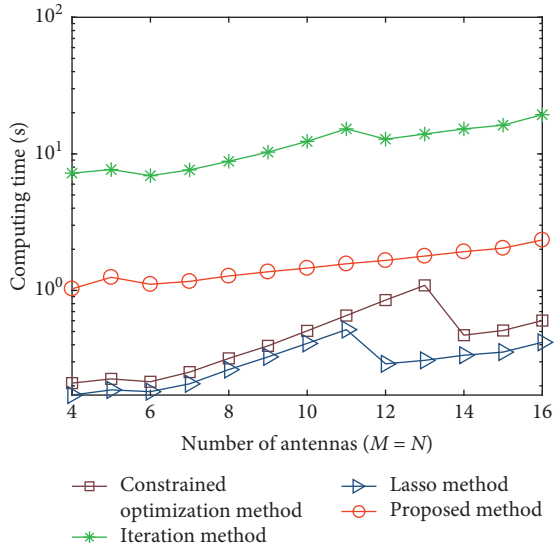

Figure 3: Computing time of the methods against the number of antennas when SNR = 20 dB.

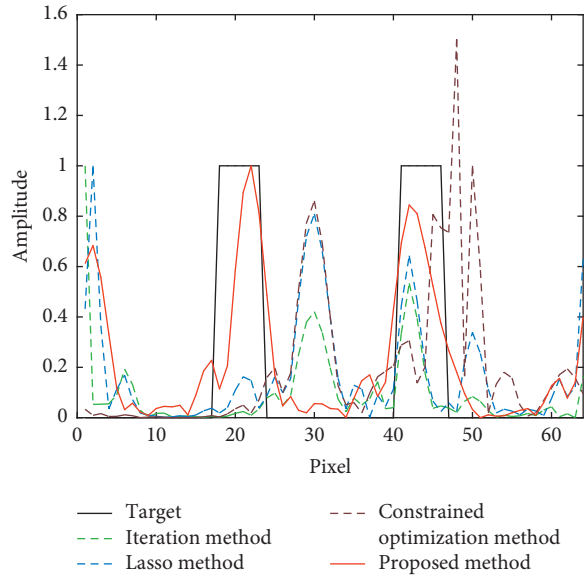

Figure 4: Sparse recovery results of one range of target with the constrained optimization method [14], iterative method [15], Lasso method, and proposed method ($M = N = 15$, SNR = 20 dB, $\gamma = 15$, and $\rho = 0.2$).

range is a one-dimensional two-slit image. The number of Monte Carlo trails is 500 in all simulations. All the simulations are run using MATLAB 2014a in a computer with the following configuration: Intel(R) Core (TM) i7-7700CPU 3.6 GHz and 16 GB memory.

The convergence of our algorithm is shown in Figure 2. It illustrates the MSE of the reconstruction results with iteration numbers i and k. Normally, the algorithm converges within $i = 60$ and $k = 150$.

Figure 3 shows the computation time of each algorithm with different numbers of antennas. It can be seen that the proposed method takes less time than the iterative method in [15] but takes longer time than the constrained optimization method [14] and Lasso method.

Figure 4 shows the results of the image recovery by using different methods. It can be seen in Figure 4 that the iterative method [15] and Lasso method work slightly better than the constrained optimization method [14] and the proposed method achieves much better performance than the iterative method [15] and Lasso method. Simulations show that the MSEs of the constrained optimization method [14], the iterative method [15], the Lasso method, and the proposed method are 14.93, 11.07, 12.40, and 4.78, respectively.

Figure 5 shows the MSE and PRC of the four methods, where the error parameter ε changes from 0.2 to 0.8 with the interval 0.02. We can see that the MSE of the proposed method is much smaller than that of the other three methods

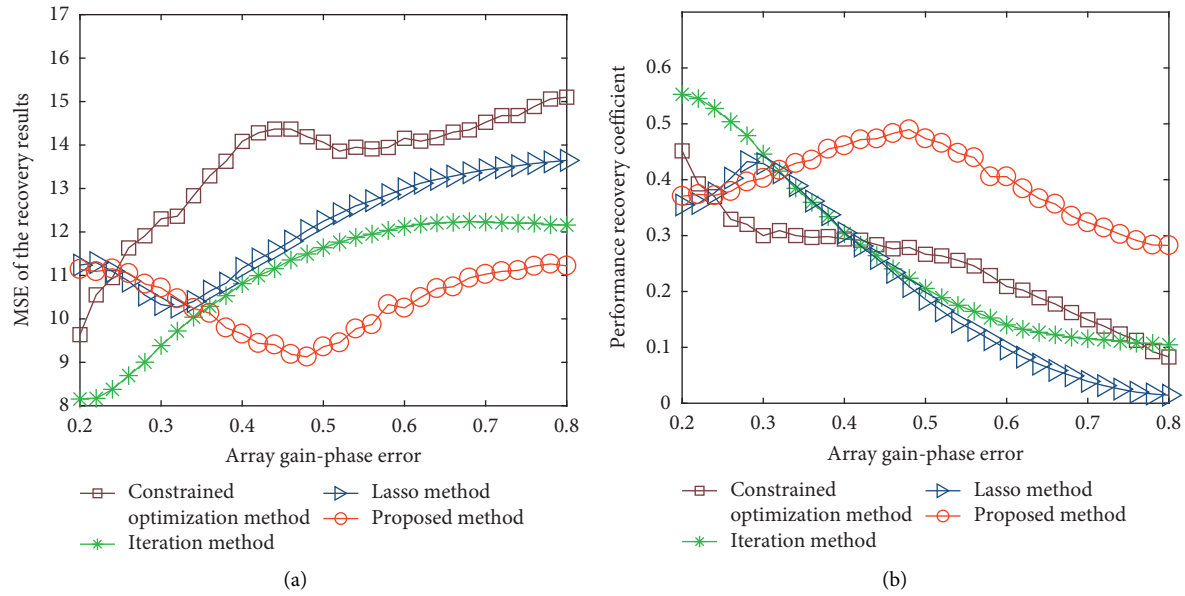

FIGURE 5: MSE and PRC of the sparse recovery results with the constrained optimization method [14], iterative method [15], Lasso method, and proposed method with different array gain-phase errors ($M = N = 15$, SNR = 20 dB, $\gamma = 15$, and $\rho = 0.2$). (a) MSE of the sparse recovery results with different array gain-phase errors. (b) PRC of the sparse recovery results with different array gain-phase errors.

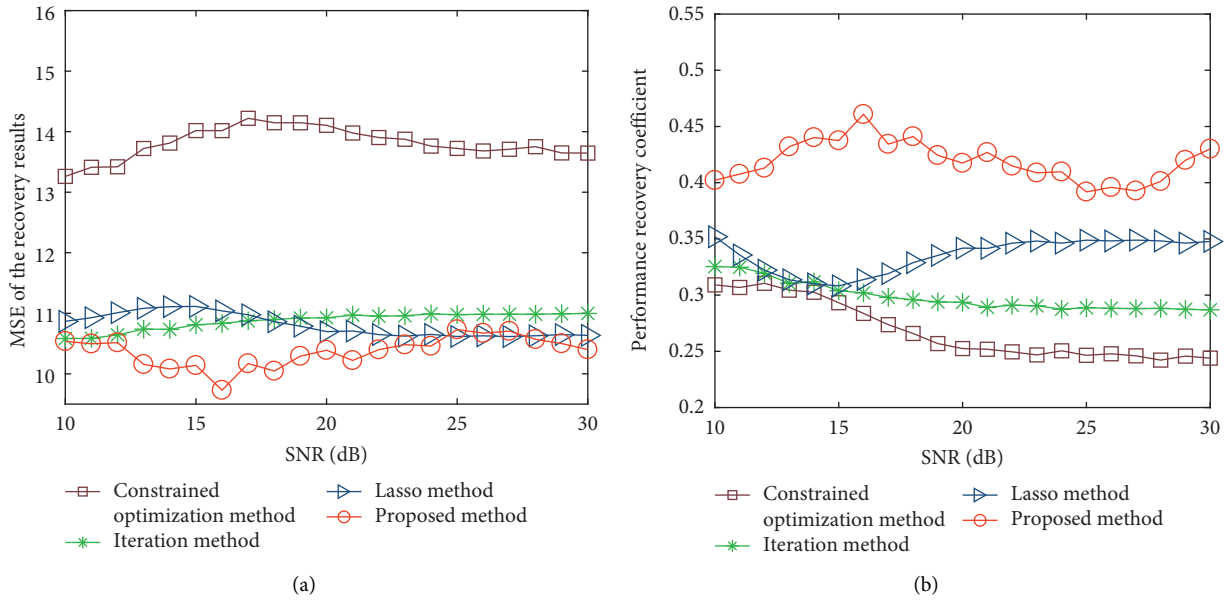

FIGURE 6: MSE and PRC of the sparse recovery results with the constrained optimization method [14], iterative method [15], Lasso method, and proposed method with different SNRs ($M = N = 15$, $\gamma = 15$, and $\rho = 0.2$). (a) MSE of the sparse recovery results with different SNRs. (b) PRC of the sparse recovery results with different SNRs.

and the PRC is much higher than that of the other three methods when the array gain-phase error is greater than 0.35. However, the iterative method [15] and Lasso method are better than the proposed method with small errors. The proposed method achieves better sparse recovery results than others with one snapshot. As we can see from Figure 5, the proposed method is robust to array errors in the case of one snapshot.

It is indicated in Figure 6 that the performance of the proposed method is much better than that of the other three methods. As the SNR increases, better sparse recovery results can be obtained. The SNR changes from 10 dB to 30 dB with the interval 1 dB.

Figure 7 displays the effect of the regularization parameter γ and penalty parameter ρ on the MSE of the recovery results. The penalty parameter ρ is set as 0.2 in

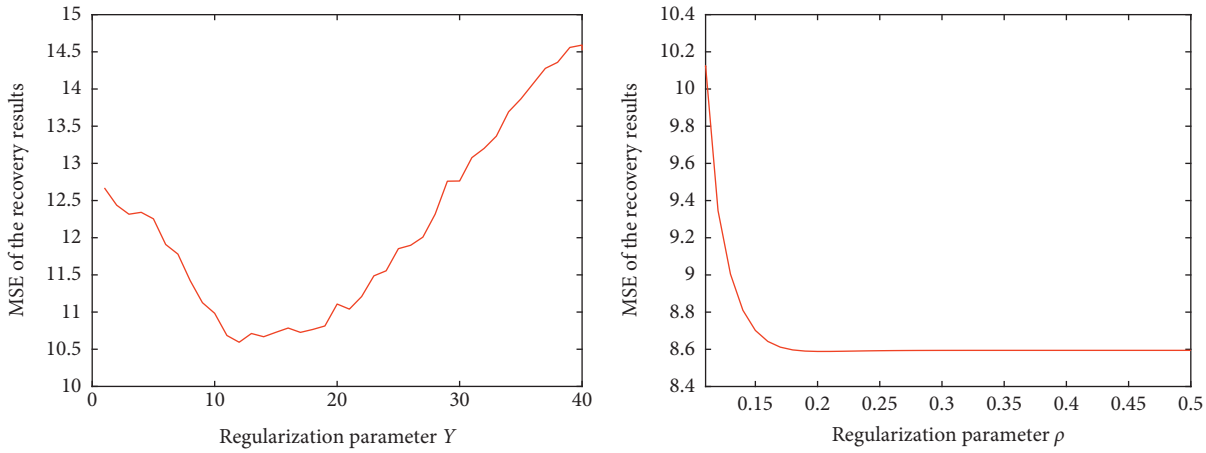

FIGURE 7: Effect of the regularization parameter γ and penalty parameter ρ on the MSE of the recovery results. (a) Convergent curve ($\rho = 0.2$). (b) Convergent curve ($\gamma = 15$).

Figure 7(a) and γ changes from 0 to 40. We set $\gamma = 15$ in Figure 7(b) and ρ changes from 0.1 to 0.5. It can be observed that the MSE decreases with the increase of γ and ρ, but when γ is too large, the algorithm will diverge.

5. Conclusions

In this work, we have investigated a robust sparse recovery-based transmit-receive angle imaging method for the bistatic MIMO radar. Signals are transformed into a sparse domain by discrete wavelet transform, and the reconstruction is achieved by a robust iterative algorithm. The proposed method is more robust to deal with the imperfection of array gain-phase errors and noise in the bistatic MIMO radar system. Simulation results have been provided to show the superiority of the proposed method, which can achieve significantly better PRC and MSE than existing methods.

Data Availability

The simulation data used to support the findings of this study are included within the article.

Conflicts of Interest

The authors declare that they have no conflicts of interest.

Acknowledgments

This study was supported by the Key Research and Development Program of Shaanxi (Program No. 2019ZDLGY09-04). It was also partially supported by the Fund for Foreign Scholars in University Research and Teaching Programs (the 111 Project; no. B18039).

References

[1] A. Haimovich, R. Blum, and L. Cimini, "MIMO radar with widely separated antennas," *IEEE Signal Processing Magazine*, vol. 25, no. 1, pp. 116–129, 2008.

[2] J. Li and P. Stoica, "MIMO radar with colocated antennas," *IEEE Signal Processing Magazine*, vol. 24, no. 5, pp. 106–114, 2007.

[3] H. Yan, J. Li, and G. Liao, "Multitarget identifcation and localization using bistatic MIMO radar systems," *EURASIP Journal on Advances in Signal Processing*, vol. 2008, Article ID 283483, 8 pages, 2008.

[4] C. Zhou, Y. Gu, S. He et al., "A robust and efficient algorithm for coprime array adaptive beamforming," *IEEE Transactions on Vehicular Technology*, vol. 67, no. 2, pp. 1099–1112, 2017.

[5] C. Shi, F. Wang, M. Sellathurai, J. Zhou, and S. Salous, "Low probability of intercept-based optimal power allocation scheme for an integrated multistatic radar and communication system," *IEEE Systems Journal*, pp. 1–12, 2019.

[6] C. Shi, F. Wang, S. Salous, and J. Zhou, "Joint subcarrier assignment and power allocation strategy for integrated radar and communications system based on power minimization," *IEEE Sensors Journal*, vol. 19, no. 23, pp. 11167–11179, 2019.

[7] E. Fishler, A. Haimovich, R. Blum, L. Cimini, D. Chizhik, and R. Valenzuela, "MIMO radar: an idea whose time has come," in *Proceedings of the 2004 IEEE Radar Conference*, pp. 71–78, Philadelphia, PA, USA, April 2004.

[8] E. Fisher, A. Haimovich, R. Blum, L. Cimini, D. Chizhik, and R. Valenzuela, "Spatial diversity in radars—models and detection performance," *IEEE Transactions on Signal Processing*, vol. 54, no. 3, pp. 823–838, 2006.

[9] I. Bekkerman and J. Tabrikian, "Target detection and localization using MIMO radars and sonars," *IEEE Transactions on Signal Processing*, vol. 54, no. 10, pp. 3873–3883, 2006.

[10] J. L. Chen, "A method for fast multi-target localization in bistatic MIMO radar system," *Journal of Electronics & Information Technology*, vol. 31, no. 7, pp. 1664–1668, 2009.

[11] J. Li, Y. Guo, G. Liao, Q. Guo, and J. Xi, "Dimension reduced sparse recovery method for clutter suppression in bistatic MIMO radar," in *Proceedings of the 2015 IEEE Radar Conference*, Washington DC, USA, May 2015.

[12] G. Zheng, D. Zhang, Y. Zhang, J. Tang, C. Feng, and X. Hu, "Fast OMP algorithm for 3D parameters super-resolution estimation in bistatic MIMO radar," *Electronics Letters*, vol. 52, no. 13, pp. 1164–1166, 2016.

[13] N. Tong, Y. Zhang, G. Hu, X. He, and X. Hu, "Multiple-input–multiple-output radar super-resolution three-dimensional imaging based on a dimension-reduction compressive

sensing," *IET Radar, Sonar & Navigation*, vol. 10, no. 4, pp. 757–764, 2016.

[14] J. Li, S. Zhu, X. Chen, L. Lv, G. Liao, and M. Yi, "Sparse recovery for bistatic MIMO radar imaging in the presence of array gain uncertainties," *International Journal of Antennas and Propagation*, vol. 2014, Article ID 807960, 6 pages, 2014.

[15] Z. Liu, J. Li, J. Chang, and Y. Guo, "A compressive sensing-based bistatic MIMO radar imaging method in the presence of array errors," *International Journal of Antennas and Propagation*, vol. 2018, Article ID 9434360, 6 pages, 2018.

[16] J. Chen, H. Gu, and W. Su, "A new method for joint DOD and DOA estimation in bistatic MIMO radar," *Signal Processing*, vol. 90, no. 2, pp. 714–718, 2010.

[17] M. Jin, G. Liao, and J. Li, "Joint DOD and DOA estimation for bistatic MIMO radar," *Signal Processing*, vol. 89, no. 2, pp. 244–251, 2009.

[18] Y. Chi, L. L. Scharf, A. Pezeshki, and A. R. Calderbank, "Sensitivity to basis mismatch in compressed sensing," *IEEE Transactions on Signal Processing*, vol. 59, no. 5, pp. 2182–2195, 2011.

[19] H. Zhu, G. Leus, and G. B. Giannakis, "Sparsity-cognizant total least-squares for perturbed compressive sampling," *IEEE Transactions on Signal Processing*, vol. 59, no. 5, pp. 2002–2016, 2011.

[20] J. Li, P. Stoica, and Z. Wang, "Doubly constrained robust Capon beamformer," *IEEE Transactions on Signal Processing*, vol. 52, no. 9, pp. 2407–2423, 2004.

[21] S. Boyd, N. Parikh, E. Chu et al., "Distributed optimization and statistical learning via the alternating direction method of multipliers," *Foundations and Trends in Machine Learning*, vol. 3, no. 1, pp. 1–122, 2010.